JARO 2/1: 041–053 (2001)
DOI: 10.1007/s101620010027

JARO
Journal of the Association for Research in Otolaryngology

Tonotopic Projections of the Auditory Nerve to the Cochlear Nucleus Angularis in the Barn Owl

CHRISTINE KÖPPL

Institut für Zoologie, Technische Universität München, 85747 Garching, Germany

Received: 14 February 2000; Accepted: 1 November 2000; Online publication: 23 March 2001

ABSTRACT

The nucleus angularis (NA), one of the two cochlear nuclei of birds, plays an important role in the processing of sound intensity. To begin investigating the NA in detail in the barn owl, which is a popular animal model for neural mechanisms of sound localization, a frequency map for this nucleus is presented here. Focal injections of horseradish peroxidase or neurobiotin were placed either in the NA or in the cochlear nucleus magnocellularis, labeling small groups of auditory nerve fibers of known characteristic frequency (CF) from 0.25 to 9.6 kHz. The courses of their axonal branches were used to construct a composite average map of the tonotopic frequency representation in the nucleus angularis. Nucleus angularis in the barn owl, as seen in frontal sections, resembles a sheet of cells bent approximately into an S shape. The lowest frequencies were found represented at the ventromedial extreme. The representation of increasingly higher frequencies then followed the S shape, with the highest frequencies located at the ventrolateral tip. Auditory nerve fibers of a given CF always entered the nucleus angularis within a well-restricted area and then traveled along their isofrequency band within the NA while branching off terminals. The isofrequency bands were typically slanted from caudo–ventro–medial to rostro–dorso–lateral. The basic tonotopic organization is comparable to that found in other birds, the major differences being the large size and unusual shape of the barn owl's nucleus angularis.

Keywords: hearing, auditory nerve, bird, intensity coding

Correspondence to: Dr. Christine Köppl • Institut für Zoologie • Technische Universität München • Lichtenbergstrasse 4 • 85747 Garching • Germany. Telephone: 49 89 2891 3671; fax: 49 89 2891 3674; email: Christine.Koeppl@bio.tum.de

INTRODUCTION

The avian cochlear nucleus complex shows two principal subdivisions, the nucleus magnocellularis (NM) and the nucleus angularis (NA). Afferent auditory nerve fibers from the basilar papilla or cochlea split into two principal collaterals terminating in the NM and NA (review in Carr 1992). This dichotomy also represents a functional division between the two cochlear nuclei and, following them, two largely separate brainstem pathways. The two pathways have been most convincingly demonstrated in the barn owl and are dedicated to the extraction of interaural time and intensity difference, respectively, two main cues for sound localization (e.g., Takahashi et al. 1984).

NM forms the starting point of the "time pathway" and functions predominantly as a relay for the phase-locked responses of the auditory nerve, setting up their binaural convergence and thus the first computation of interaural time difference at the next-higher level (e.g., Carr 1993a). Its specialized and relatively uniform cellular structure has made it a popular and well-studied system for neural mechanisms in fast temporal processing (e.g., Carr 1993b; Trussell 1997). NA, on the other hand, forming the starting point for the "intensity pathway," appears to be much more complex than NM in both morphology and function. Several neurone types and different, sometimes complex, physiological response patterns have been described (Boord and Rasmussen 1963; Hotta 1971; Sachs and Sinnott 1978; Sullivan 1985; Warchol and Dallos 1990; Häusler et al. 1999). However, it is presently not clear how morphology and physiology relate to each other. Another important question is whether and how different types of neurones may relate to different frequency ranges.

To begin investigating the NA in more detail, a

frequency map for this nucleus in the barn owl, derived through labeling small groups of auditory nerve fibers and charting their termination sites, is presented here. The aim is to extend previous, more fragmentary data (Sullivan and Konishi 1984; Carr and Boudreau 1991) into a complete map covering the entire hearing range of the barn owl. This forms an essential basis for interpreting the distribution of neuronal cell types in the barn owl's NA, as described in a companion paper (Soares and Carr, 2001).

MATERIAL AND METHODS

Experiments were performed on 15 adult barn owls (*Tyto alba guttata*), 7 males and 8 females, from our own breeding colony. Different results from the same experiments were also used in a parallel study; therefore, details regarding anesthesia, surgery, electrophysiology, acoustic stimulation and histology can be found in Köppl et al. (1993) and will only be summarized here.

The owls were anesthetized with a combination of ketamine and xylazine (4 mg/kg and 3 mg/kg initial dose, respectively). Recordings of multiunit activity were made with HRP-filled glass micropipettes (30% HRP; external tip diameters typically 14 μm, impedance 11 MΩ) introduced through the cerebellar flocculus into the auditory brainstem. Acoustic stimuli were delivered through a closed, calibrated system in each ear. Recording sites were identified according to stereotaxic coordinates and known physiological criteria (e.g., Takahashi et al. 1984; Köppl 1997a). While the electrode was advanced, the characteristic frequency (CF), i.e., the frequency of stimulation that produces a detectable response at the lowest sound pressure level, was determined at regular depth intervals, usually 100 μm. At selected recording sites, HRP was deposited iontophoretically by passing 0.2–3.6 μA DC + for 7–20 minutes, resulting in products between 4 and 40 μA min. Up to three sites were marked on one side of the brainstem, with CFs differing by at least one octave. Following a survival time of 8 hours to 2 days, the owls were sacrificed by an anesthetic overdose and their tissues fixed by transcardial perfusion of 1% paraformaldehyde and 2.5% glutaraldehyde in 0.1M phosphate buffer. The brain was dissected free and the relevant part sectioned on a cryotome (75 μm section thickness). The section plane was orthogonal to the rostrocaudal axis, which was, in turn, defined by the long axis of the brain (Fig. 1A). The sections were processed to visualize the HRP label, by a cobalt-intensified diaminobenzidine reaction, and counterstained with neutral red. The cochleae were also dissected free and processed as whole mounts. In one animal, 5% neurobiotin was used as the tracer and visualized according to an avidin–HRP protocol described in Köppl and Carr (1997).

To document the labeling pattern, camera-lucida drawings of the brainstem and relevant nuclear outlines were first made from every section at low magnification. The drawings were then enlarged and labeled stuctures added at higher magnification. In most cases, the drawings were digitized via a graphics tablet interface connected to a personal computer, and those drawings were used for computer-assisted 3D reconstructions. Visualization of the labeling patterns from different viewing angles was thus possible, and comparisons between different brains were greatly facilitated. Data from different brains were combined by normalizing the coordinates of the extent of the label in each section to the total dorsoventral and mediolateral extent of the NA in that section and projecting these normalized coordinates onto the outline of one typical NA at the equivalent rostrocaudal position. Three-dimensional reconstructions of the combined data were then viewed from different angles and isofrequency lines defined along the estimated medians, i.e., the densest labeled parts of labeled bands. In cases of several closely lying bands of similar CF, individual lines were eliminated and replaced by subjective averages. This resulted in the frequency map shown in Figure 1 which contains 10 isofrequency lines. Finally, volumes occupied by different frequencies were estimated for this composite NA. For 28 positions along the rostrocaudal extent of the NA (corresponding to individual sections of the original nucleus whose outline was used), the areas demarcated by isofrequency bands (i.e., by CFs up to 0.25 kHz, 0.6 kHz, and so forth, up to the full nuclear volume) were calculated, multiplied with the section thickness, and summed over all positions.

RESULTS

Interpretation of label pattern

A total of 27 tracer injections, with 15 injected into NA, 10 into NM, and two into areas of predominantly auditory nerve, were used to construct the frequency map of NA reported here. Their CFs, determined immediately before iontophoresis, varied from 0.25 to 9.6 kHz (Table 1). Injection sizes were well restricted, such that frequency-specific uptake of the tracer could be assumed. The diameter of the area of extracellular tracer reaction product visible in the brain sections was typically 300–400 μm (Table 1). Serial drawings and reconstructions (see Materials and Methods section) were used to identify the VIIIth nerve label and separate it from efferent fiber tracts originating in the NA or NM, respectively, depending on the injection

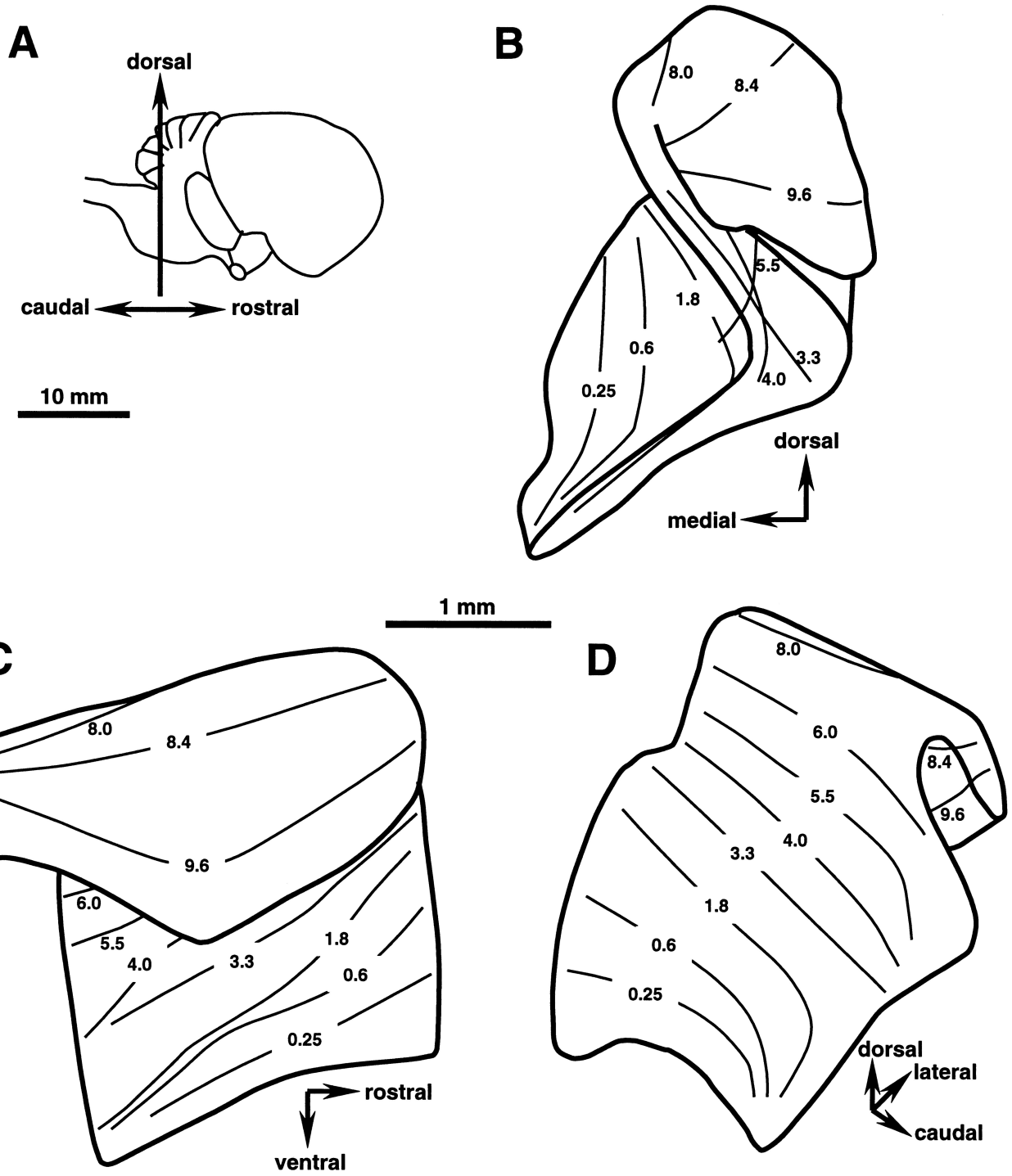

FIG. 1. **A**. Simplified drawing of a barn owl's brain as seen from the right side. The vertical arrow also marks the plane of sectioning used in this study. **B–D**. Schematic three-dimensional reconstructions of the NA and its tonotopic organization from 3 different viewing angles (given by the orienting arrows). The outline of the nucleus is drawn using thick lines. The thin lines within mark the centers of different isofrequency bands, and the respective frequencies are given in kHz. The scale bar in the middle of the figure applies to **B–D**. Note, however, that the scale bar applies only to planar structures and thus can not be used to measure distances along curved surfaces in the 3D views.

site. Only projections which, as a group, could be followed peripherally, thus confirming that the fibers originated in the basilar papilla, were used for the frequency map described here. Special care was taken in the cases of CFs below 1 kHz, and the nerve branches innervating the adjacent lagenar macula (a vestibular organ) were also scrutinized for labeled fibers in the cochlear whole mount. In only one case was a small

TABLE 1

Parameters of tracer injections[a]

Animal/side	*Injection site*	*CF (Hz)*	*Tracer*	*r-c extension (μm)*	*Maximum diameter (μm)*
Tyto 25 L	NA	250	HRP	375	300
Tyto 22 R	NA	270	HRP	375	247
Tyto 25 R	NA	480	HRP	825	1013
Tyto 24 R	NA	600	HRP	150	184
Tyto 24 L	NA	640	HRP	75	132
Tyto 31 R	NM (nVIII)	1000	HRP	300	300
Tyto 30 R	NM (nVIII)	1100	HRP	300	350
Tyto 20 R	NM	1750	HRP	150	82
Tyto 23 R	NA	1790	HRP	375	317
Tyto 21 L	NA	1940	HRP	225	161
Tyto 26 R	NM	3300	Neurobiotin		
Tyto 19 R	next to NA	3360	HRP	375	348
Tyto 17 R	NM	3430	HRP	375	733
Tyto 15 L	NM	3600	HRP	150	154
Tyto 22 R	NA	4080	HRP	225	204
Tyto 19 L	NM	4140	HRP	300	528
Tyto 17 L	NM	4600	HRP	375	885
Tyto 25 R	NA	5290	HRP	300	207
Tyto 16 R	NM	5300	HRP	450	944
Tyto 23 R	NA	5600	HRP	225	242
Tyto 14 L	NM	5660	HRP	225	289
Tyto 32 R	nVIII	6000	HRP	150	250
Tyto 16 L	NA	7700	HRP	750	642
Tyto 22 R	NA	8050	HRP	225	151
Tyto 16 R	NA	8400	HRP	450	336
Tyto 19 L	NA	9000	HRP	375	237
Tyto 19 R	NA	9600	HRP	675	425

[a]Parameters of all the tracer injections, sorted according to CF (column 3). The first column gives the individual animal code and the side of injection (L = left, R = right). The injection site (column 2) was mostly in the NA or the NM, in some cases in the auditory nerve layer (nVIII) or on the borders of the NM or the NA, straddling areas of predominantly auditory nerve fibers. The last two columns give two measures of the size of the injections, the rostrocaudal extension (calculated from the number of sections) and the maximal diameter of the area of extracellular reaction product in any one section (not corrected for tissue shrinkage). In the one case where neurobiotin was used, no sizes are given, since this tracer is not demonstrable extracellularly after the survival time used.

minority of labeled fibers (3 of about 60) seen traveling toward the lagenar macula. This injection was among the largest reported here (Tyto 25R at 480 Hz; see Table 1 and Fig. 2B) and may have included some areas surrounding the target center in NA.

Uptake of the tracer by VIIIth nerve terminals and fibers regularly resulted in the apparently complete labeling of the respective VIIIth nerve arbors in both cochlear nuclei. An VIIIth nerve label within the NA was included in the present analysis, aiming for a

FIG. 2. Camera-lucida drawings of the labeling pattern observed in the right half of three different brains (**A–C**) with a range of injection sizes. For each brain, 4 representative sections along the rostrocaudal extent of the NA are shown, at the positions indicated as percentages from NA's caudal end. Outlines of the NA, the brainstem, and, in some panels, truncated outlines of the nucleus laminaris are provided (for general orientation, see Fig. 1). Although all the label that was observed is drawn, the area shown is restricted to the immediate surroundings of the NA, which contained almost exclusively auditory nerve label (some NA efferent fibers can be seen heading ventrally in all most-rostral panels) (**A** 81%, **B** 81%, and **C** 87%). Medial is to the left, dorsal to the top; the scale bar in **A** (81%) applies to all panels. **A**. Tyto 16R (see also Table 1), where one injection was placed at a 5.29-kHz site in the NM (injection site not shown) and a second one at an 8.4-kHz site in the NA (cross-hatched area). The lower band of label in the NA was traced to the 5.29-kHz injection; the label around the most dorsal region of the NA to the 8.4-kHz injection. **B**. Tyto 25R, with two injections in the NA: a large one at 480 Hz (its center at the ventral edge of the NA is indicated in solid black; the area of dense extracellular reaction product is shown cross-hatched) and a smaller one at 5.3 kHz (again shown in solid black, with some diffusion of the label along the electrode track into areas of higher CF). Note that although the label resulting from the two injections was not strictly separable in every section, the center of the 5.3-kHz label is comparable to the label shown in **A**, from a 5.29-kHz site in the NM. **C**. Tyto 19R, with one injection at a 9.6-kHz site in the NA (center of injection not shown) and a small second one at 3.36 kHz (indicated in solid black) just outside the NA, in an area of auditory nerve and of NA output fibers. The 9.6-kHz label was consistently restricted to the ventro lateral tip of the NA. In the most rostral section shown, NA output fibers from this region are very prominent and can be seen running lateral and ventral of the NA. Labeled terminals at more ventral sites within the NA were consistent with being auditory nerve fibers labeled from the 3.36-kHz site.

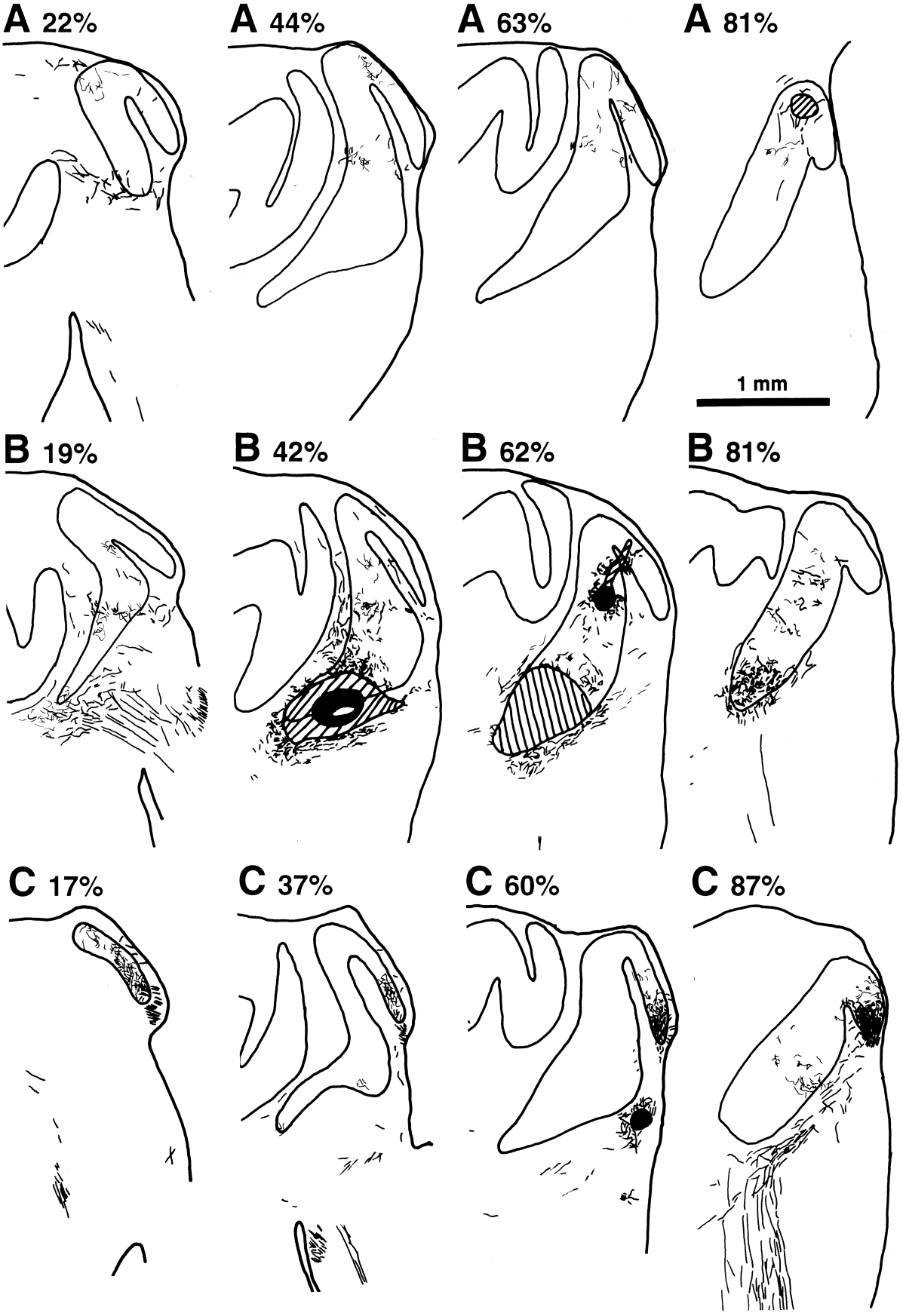
A 22%
A 44%
A 63%
A 81%
1 mm
B 19%
B 42%
B 62%
B 81%
C 17%
C 37%
C 60%
C 87%

description of the general position of isofrequency projections rather than a strict distinction between fibers and terminals. Furthermore, in the absence of any ultrastructural data on the avian NA, it cannot be excluded that en-passant synapses may be a significant proportion of the synaptic contacts made by VIIIth nerve fibers.

General shape of the nucleus angularis

The NA in the barn owl has a somewhat unusual and complex shape. It is situated at the dorsolateral extreme of the brainstem and extends for about 2.3 mm in the rostrocaudal dimension (not corrected for tissue shrinkage). In serial cross sections of the brainstem, it is first encountered caudally as a small band of cells forming a bulge above and lateral to the auditory nerve (Fig. 3A). Followed rostrally, it quickly expands to form an inverted U shape (Fig. 3B). The medial arm then elongates greatly and develops a prominent foot extending medially at an angle, such that the whole nucleus appears bent into an S shape (Fig. 3C). In the rostral half of NA's extent, the medial arm expands considerably, while the lateral arm remains slim (Fig. 3D). The lateral arm then shortens first, giving the NA an almost linear, rodlike shape in its most rostral cross sections (Fig. 3E). Reconstructing its three-dimensional shape, the NA is basically a sheet of cells into an S shape (see Fig. 1).

The terminal areas of auditory nerve fibers of different characteristic frequency

Both the position of the injection sites in the NA and the position of labeled VIIIth nerve arborizations within the NA were systematically correlated with the CF determined immediately before iontophoresis. The labeling was typically restricted to a band of VIIIth neve fibers and terminals running along most of the rostrocaudal extent of the NA. No difference was noted in the position of the label originating from injection sites in the NA or the NM, respectively, at comparable CFs. A range of examples for the label obtained is illustrated in Figures 2 and 4. Figure 4 shows micrographs of a case where 3 injections covering a wide range of CFs were placed in one NA, convincingly demonstrating the tonotopic order. Figure 2 shows, in more schematic form, the results of an additional 6 injections in 3 different brains, including a comparison of injections into the NA (Fig. 2B) and the NM (Fig. 2A) at the same CF. The composite tonotopic map (see Materials and Methods section) is illustrated in Figure 1 and followed the oblique axis of the NA's S shape. Fibers of the highest CFs labeled (9 and 9.6 kHz) terminated at or near the ventral tip of the lateral arm of the NA. Fibers of 8.4 kHz CF terminated dorsally further along the NA's lateral arm. The label at 8.0- and 7.7 kHz CFs extended into the dorsal bend of the NA. Progressively lower frequencies were represented at increasingly ventromedial positions along the medial arm of the NA. The isofrequency bands were typically slanted from caudo–ventro–medial to rostro–dorso–lateral. This slant appeared more pronounced the lower the frequency was (Fig. 1).

To obtain a semiquantitative description of the frequency distribution within the NA, the cumulative NA volume with increasing frequencies was estimated (see Materials and Methods section), assuming an upper CF limit of 10 kHz. This was well fit by a simple linear regresion (Fig. 5A), which was then used to estimate volumes per octave around arbitrary center frequencies. As is shown in Figure 5B, the volume per octave steadily and linearly increased with increasing CF.

Course of auditory nerve fibers towards the nucleus angularis

Auditory nerve fibers of a given CF always entered the NA within a well-restricted area covering a few hundred micrometers along the rostrocaudal extension of the nucleus. Label within the NA, however, usually extended over its full rostrocaudal dimension. It thus appears that, having entered the NA, individual fibers branch off terminals as they travel along their isofrequency band. Indeed, the label seen within the NA was typically a mixture of fibers and terminals or an alternation of both in successive sections.

The tonotopic organization of auditory nerve projections was also evident in their course toward the nucleus. After passing through the internal auditory meatus, the compact auditory nerve spirals (Köppl 1997b), and then fans out into a thick sheet of fibers. Fibers of the lowest CFs entered the brainstem at the rostral extreme of the auditory nerve sheet. After splitting off the collaterals that headed far caudally for the NM, they entered the NA at the ventral and lateral extreme of its foot section (Fig. 4B,E, 2B; 19%). Fibers of medium CFs (3–5 kHz) entered the brainstem near

FIG. 3. Typical cross sections of the brainstem of the barn owl, within the region of the nucleus angularis (NA), where **A** is the most caudal and **E** the most rostral section. Successive sections are separated by 450 μm, except for **A** and **B**, which are only 300 μm apart; the relative positions of **A–E** are at 17%, 30%, 50%, 70%, and 90% of NA's total extent. The left series of panels shows images taken by a video camera and framegrabber board; the scale bar in **A** applies to all. The right series of panels shows mirrored drawings from the same sections, outlining the NA in black and the nucleus magnocellularis (NM), the nucleus laminaris (NL), and the brainstem in gray.

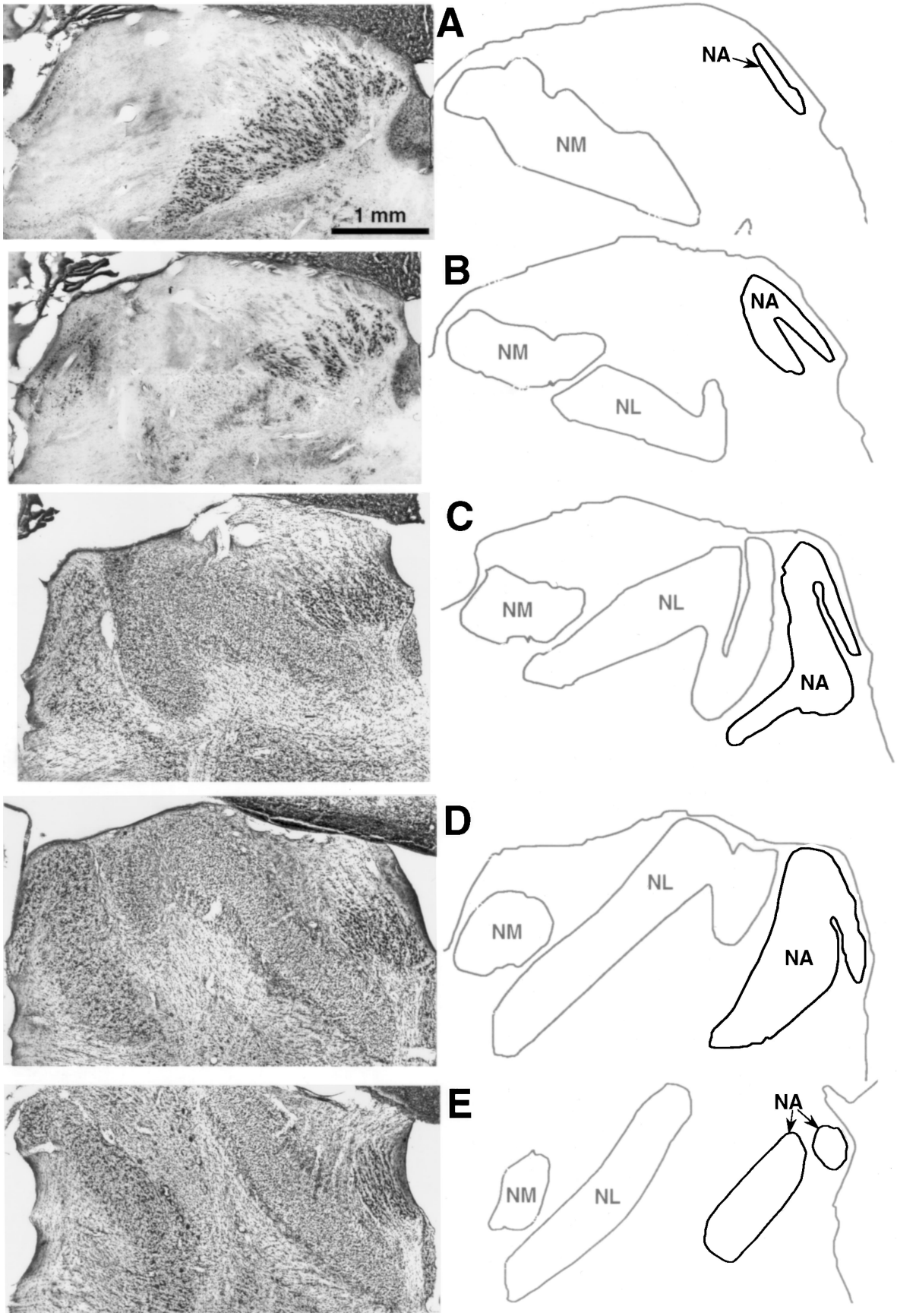
A
NA
NM
1 mm
B
NA
NM
NL
C
NM
NL
NA
D
NL
NM
NA
E
NA
NM
NL

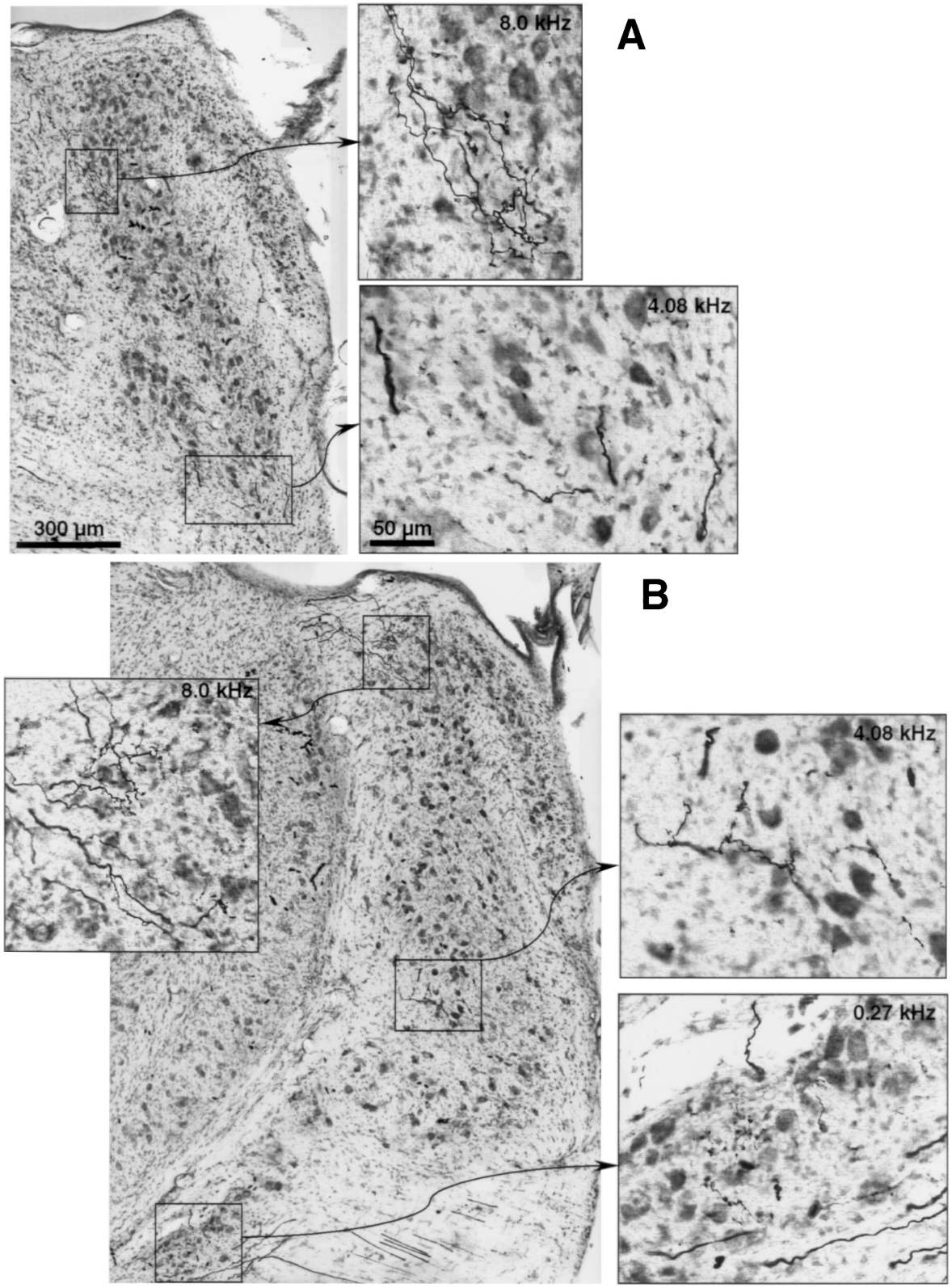

FIG. 4. Labeling pattern in an individual owl that received three HRP injections into one NA at sites with CFs of 8.0, 4.08, and 0.27 kHz. **A–D**. Cross sections of the NA at increasingly rostral positions at 26%, 42%, 61%, and 87% of NA's total extent. Each panel shows the complete NA at low magnification and one to three enlargements of labeled areas, as indicated by boxes and arrows. The CF of the injection site from which the label originated is also indicated in each case. Two of the injection sites are shown in **C**. The scale bars given in **A** apply to all low- and high-magnification images, re-

(continued on next page)

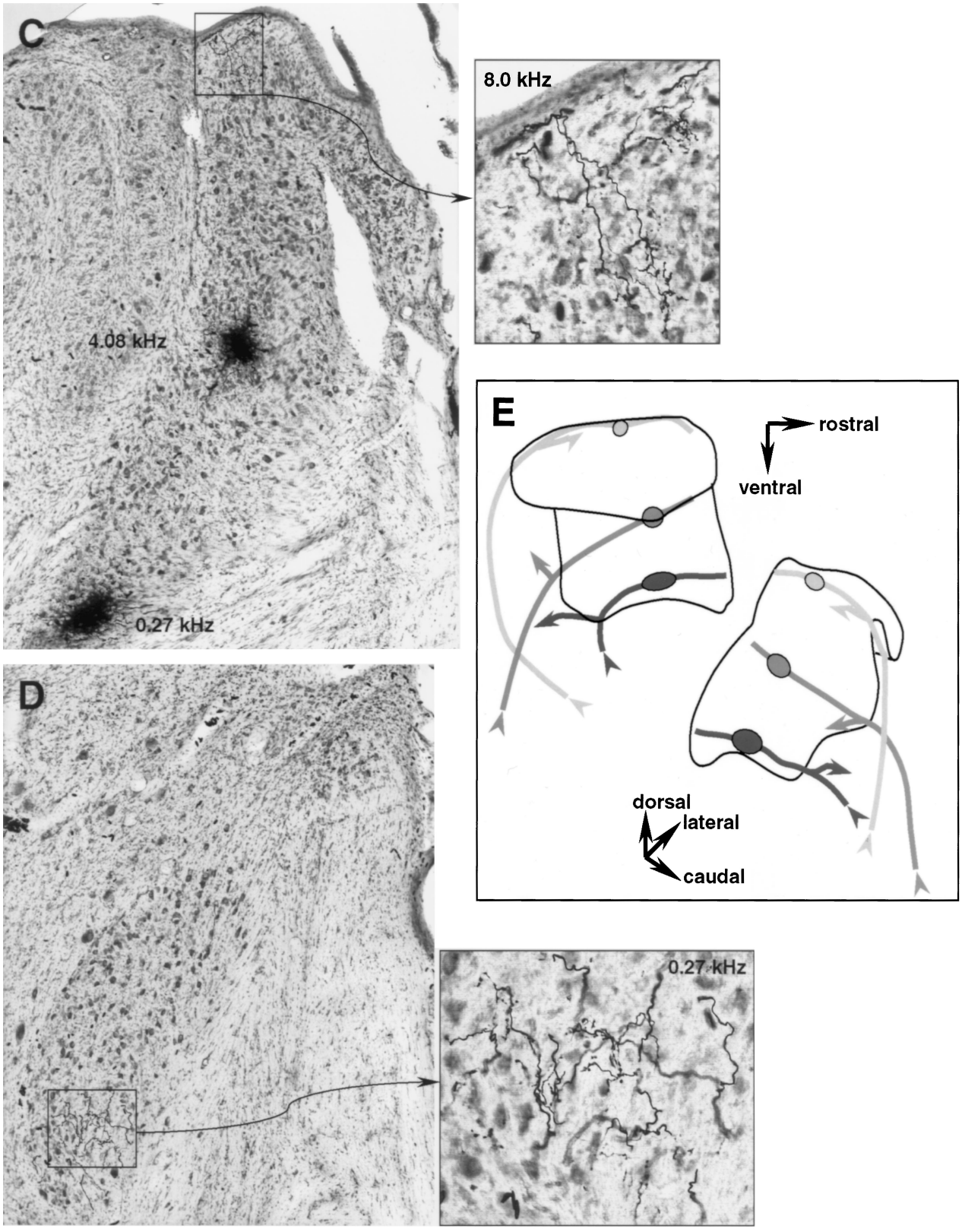

spectively. **E**. Schematic summary of the labeling pattern to illustrate the typical course of auditory nerve fibers of different CF. Two different views of a three-dimensional reconstruction of the NA, outlined by thin black lines, are drawn. The three injection sites are indicated as oval shapes in different shades of gray and the fiber tracts labeled by them in corresponding shades (dark gray: CF = 0.27 kHz; medium gray: CF = 4.08 kHz; light gray: CF = 8.0 kHz). Arrowheads in corresponding shades of gray help to identify the entry points into the brainstem as well as the collaterals headed for the nucleus magnocellularis, which are shown truncated.

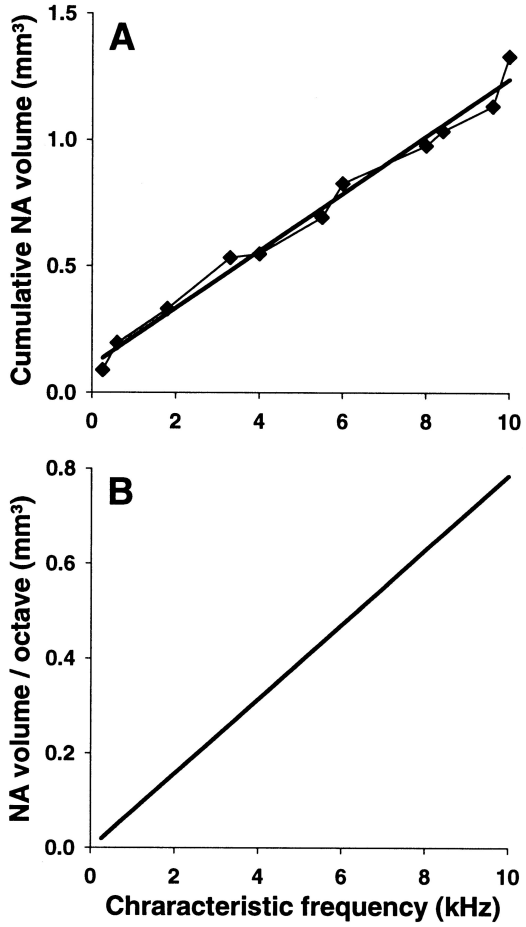

FIG. 5. Frequency distribution in the NA. **A**. Cumulative volume as a function of characteristic frequency. The symbols joined by a thin line indicate values derived from a typical NA into which the composite map was projected (see Materials and Methods section). The thick line is a linear regression fit that was used to calculate the data shown in panel **B** ($n = 11$, $r = 0.933$, $p < 0.001$). **B**. Estimates of the volumes devoted per octave at different center frequencies. Note the steady increase in volume indicating that the representation in the NA is biased toward high frequencies.

or beyond the caudal end of NA. The collaterals headed for NA then traveled a short distance rostrally and entered NAs medial arm mainly from the lateral side (Fig. 2E). Higher-CF fibers, of 7–8.4 kHz, entered the brainstem most caudally. They also entered the NA most caudally, approaching near its top end from the dorsal and medial side (Fig. 4A,B,E, 2A; 22%). The collaterals headed for the NM split off near this entry region to the NA. An unusual feature was observed in the fibers labeled from the two highest-frequency injections (9 and 9.6 kHz). They also approached the NA at its caudal extreme but then entered the lateral arm from below and laterally Fig. 2C). Most remarkably, however, these fibers did not send any collaterals toward the NM. Both of these extreme high-frequency labels were carried out in the same individual (one on each side), and, although two further HRP injections at lower frequencies resulted in a normal labeling pattern in both cochlear nuclei in this animal, further data from different individuals are needed to establish if the observed lack of projections at the highest frequencies is typical.

DISCUSSION

Comparison with previous studies of the barn owl's nucleus angularis

The shape of the barn owl's NA was originally described as a simple inverted "U" in cross section (Takahashi and Konishi 1988), an interpretation subsequently adhered to (e.g., Carr et al. 1989; Carr and Boudreau 1991; Adolphs 1993; Levin et al. 1997). It is shown here and in a companion paper (Soares and Carr, 2001) that the medial arm of the NA has a prominent extension, protruding ventromedially and giving the nucleus more the appearance of an "S" in cross section. The tonotopic gradient described here basically followed the S shape of the cellular sheet of the NA, starting with the lowest CFs at the ventromedial foot end. These results are consistent with earlier, more fragmentary data on the NA's tonotopicity. Single-unit recordings had shown a tonotopic order from high to low frequencies along dorsoventrally oriented electrode tracks (Sullivan and Konishi 1984). The fact that the inverse tonotopicity of the NA's lateral arm was missed may be explained by its extreme lateral position which leads to it being systematically bypassed if the electrodes are aimed along the wider medial arm. Indeed, consistent with this suggestion, Sullivan and Konishi's (1984) data on the NA contained virtually no CFs above 8 kHz. Carr and Boudreau (1991) found the projection areas of auditory nerve fibers of 7 kHz around the most dorsal point in NA, with 6 and 5 kHz progressively below that along the medial arm of the NA. This is also in agreement with the data shown here.

Reconstructing several single auditory nerve fibers in the 5–7 kHz CF range, Carr and Boudreau (1991) typically observed two terminal branches forming noncontiguous terminal fields within NA. One of these fields was more rostral, dorsal, and lateral relative to the other. The direction of the isofrequency lines derived from the present multiple-label data nicely reflects this pattern seen in single fibers. As shown in Figure 1, isofrequency lines were typically slanted from caudo–ventro–medial to rostro–dorso–lateral.

Frequency representation in nucleus angularis

Our estimates of NA volume occupied per octave showed a steady expansion from the lowest to the highest frequencies and implied a strong emphasis on the

high frequencies of the barn owl's hearing range. This is consistent with previous data implicating the NA in the processing of sound intensity (Takahashi et al. 1984; Sullivan and Konishi 1984). It is well known that the owl relies on interaural intensity differences created in the vertical plane by its facial feather disk and only at high frequencies, above approximately 4 kHz, to determine the elevational coordinate of a sound source (e.g., Moiseff 1989; Knudsen and Konishi 1979). Therefore, high frequencies would be predicted to be overrepresented in any nucleus concerned with intensity processing. However, in the barn owl, high frequencies are also known to be critical for determining interaural time differences with unusually high accuracy (e.g., Takahashi et al. 1984; Köppl 1997c). Indeed, the basic importance of the high frequencies for the owl is already reflected in their cochlear representation (Köppl et al. 1993). The space devoted to different frequency ranges along the basilar papilla rises more than tenfold with increasing frequency, from about 0.5 to 8 mm/octave at 8 kHz and above. However, as shown by Köppl (1997b), the spatial representation along the basilar papilla is not identical to the neural representation in the cochlear output, i.e., to the numbers of afferent auditory nerve fibers with different CFs. The auditory nerve shows a steep increase in fiber numbers per octave from the lowest frequencies to about 3 kHz. Frequencies from 3 to 7 kHz are represented with approximately equal numbers per octave and the number of fibers then declines again for the highest frequencies (Köppl 1997b). Compared with this input, the relative volumes estimated for the different frequencies in the NA are an underrepresentation of low to medium frequencies and an overrepresentation of the upper hearing range. This overrepresentation may be even more pronounced if cell numbers are considered, since Soares and Carr (2001) have shown that cell densities in the barn owl's NA increase from the regions of low CF toward those of high CF.

Comparison with the nucleus angularis of other birds

The first thorough descriptions of the avian NA date back to early in the 20th century and were summarized and extended by Boord and Rasmussen (1963). Their basic description of the tonotopicity in the NA, based on the termination of different portions of the auditory nerve, agrees with later physiological mappings using single-unit recordings (Konishi 1970; Hotta 1971; Warchol and Dallos 1990). According to the most detailed mappings in the house sparrow by Konishi (1970), frequencies increase from rostro–medio–ventral to caudo–latero–dorsal. This organization also corresponds to that described here in the barn owl (Fig. 1). The main difference between the barn owl and other birds appears to be the large size of the owl's NA and its convoluted S shape. The avian NA is generally drawn or described as an oval-, bean-,or cap-shaped structure in cross section (e.g., Boord and Rasmussen 1963; Winter 1963; Whitehead and Morest 1981). The more complicated shape of the barn owl's NA may be derived by elongating both ends into an inverted U and further elongating the medial arm.

Cytologically, Boord and Rasmussen (1963) distinguished three subdivisions of the pigeon NA—medial, lateral, and ventrolateral. This classification was based largely on a variation in cell sizes and the probably erroneous assumption (discussed below) that the ventrolateral division received nonauditory input. A more recent study of cell types in the pigeon NA (Häusler et al. 1999) described two major subdivisions, NA medial and NA proper. Their definition of divisions was also based heavily on variations in cell sizes and density across the nucleus, but there was, in addition, evidence for more heterogeneity of cell types in the NA proper. These traditional classifications of NA cell types were questioned by Soares and Carr (2001) in a new study on the cytoarchitecture of the barn owl NA. They suggested an alternative, possibly more functional classification scheme (after Doucet and Ryugo 1997) that takes into account the dendritic orientation relative to the nucleus' tonotopic axis. Four major cell types were thus defined. While changes in cell size and density were also seen in the barn owl, this was interpreted as a secondary variation within each basic cell type and no differential distribution of cell types across the NA was thus observed (Soares and Carr, 2001).

While the avian NA thus appears to contain a variety of neurone types, it is still undecided whether the different classifications of cell types are due more to semantic differences or to a genuine species difference between pigeon and barn owl. Ultimately, it is an important functional question as to how cell types in the avian NA vary across regions of different characteristic frequency. Is there a fundamental change in neurone morphologies, correlated with different response patterns, such as shown for comparable cell types in the mammalian cochlear nucleus complex (e.g., Rhode and Greenberg, 1992)? This would suggest emphases on different computational aspects in different frequency bands. Alternatively, or in addition, minor changes, such as in soma size, could reflect changing requirements for the same neuronal computations across frequencies, as was suggested for the different parts of the NM (Köppl 1994). Response patterns in the avian NA were not reported to vary across different CFs, but large differences in the relative abundance of different response types were seen between studies on different species (Hotta 1971;

Sachs and Sinnott 1978; Sullivan and Konishi 1984; Warchol and Dallos 1990). Studies correlating neuronal morphology and physiology are needed to resolve these discrepancies and questions.

In the study of the pigeon's NA by Boord and Rasmussen (1963), the ventrolateral division was reported to receive only input from the macular lagena, a vestibular organ situated at the apical tip of the cochlear duct in all nonmammals. This vestibular projection was found adjacent to the low-frequency projections from the most apical portions of the basilar papilla. Similarly, it was claimed that a subdivision of the nucleus magnocellularis (NM, the other cochlear nucleus) received only lagenar input (Boord and Rasmussen 1963). However, more recent, careful tracer experiments failed to find any lagenar projections to the cochlear nuclei in chickens (Kaiser and Manley 1996). In addition, it was shown in the barn owl that the full extent of both the NM (Köppl 1994) and the NA (this study) receives auditory input from the basilar papilla. Therefore, it is likely that in the original axon degeneration study of Boord and Rasmussen (1963), the inclusion of some apical papillar fibers in the lagenar ablation experiment (which the authors themselves concede) led to the erroneous conclusion of lagenar input to the cochlear nuclei.

ACKNOWLEDGMENTS

I thank Otto Gleich, who participated in many of the experiments used in this report, and Catherine Carr, Otto Gleich, and Geoff Manley for commenting on earlier versions of the manuscript. Daphne Soares and Catherine Carr also generously shared unpublished material. The work was supported by a Heisenberg Fellowship to C. Köppl and a grant to G. Manley from the Deutsche Forschungsgemeinschaft within the SFB 204 "Gehör."

REFERENCES

ADOLPHS R. Acetylcholinesterase staining differentiates functionally distinct auditory pathways in the barn owl. J. Comp. Neurol. 329:365–377, 1993.

BOORD RL, RASMUSSEN GL. Projection of the cochlear and lagenar nerves on the cochlear nuclei of the pigeon. J. Comp. Neurol. 120:463–473, 1963.

CARR CE. Evolution of the central auditory system in reptiles and birds. In: Webster DB, Fay RR, Popper AN (eds) The Evolutionary Biology of Hearing, 1st ed. Springer-Verlag New York, 1992, 511–543.

CARR CE. Delay line models of sound localization in the barn owl. Am. Zool. 33:79–85, 1993a.

CARR CE. Processing of temporal information in the brain. Ann. Rev. Neurosci. 16:223–243, 1993b.

CARR CE, BOUDREAU RE. Central projections of auditory nerve fibers in the barn owl. J. Comp. Neurol. 314:306–318, 1991.

CARR CE, FUJITA I, KONISHI M. Distribution of GABAergic neurons and terminals in the auditory system of the barn owl. J. Comp. Neurol. 286:190–207, 1989.

DOUCET JR, RYUGO DK. Projections from the ventral cochlear nucleus to the dorsal cochlear nucleus in rats. J. Comp. Neurol. 385:245–264, 1997.

HÄUSLER UHL, SULLIVAN WE, SOARES D, CARR CE. A morphological study of the cochlear nuclei of the pigeon (*Columba livia*). Brain Behav. Evol. 54:290–302, 1999.

HOTTA T. Unit responses from the nucleus angularis in the pigeon's medulla. Comp. Biochem. Physiol. 40A:415–424, 1971.

KAISER A, MANLEY GA. Brainstem connections of the *Macula lagenae* in the chicken. J. Comp. Neurol. 374:108–117, 1996.

KNUDSEN EI, KONISHI M. Mechanisms of sound localization in the barn owl (*Tyto alba*). J. Comp. Physiol. A 133:13–21, 1979.

KÖPPL C. Auditory nerve terminals in the cochlear nucleus magnocellularis: Differences between low and high frequencies. J. Comp. Neurol. 339:438–446, 1994.

KÖPPL C. Frequency tuning and spontaneous activity in the auditory nerve and cochlear nucleus magnocellularis of the barn owl, *Tyto alba*. J. Neurophysiol. 77:364–377, 1997a.

KÖPPL C. Number and axon calibres of cochlear afferents in the barn owl. Auditory Neurosci. 3:313–334, 1997b.

KÖPPL C. Phase locking to high frequencies in the auditory nerve and cochlear nucleus magnocellularis of the barn owl, *Tyto alba*. J. Neurosci. 17:3312–3321, 1997c.

KÖPPL C, CARR CE. Low-frequency pathway in the barn owl's auditory brainstem. J. Comp. Neurol. 378:265–282, 1997.

KÖPPL C, GLEICH O, MANLEY GA. An auditory fovea in the barn owl cochlea. J. Comp. Physiol. A 171:695–704, 1993.

KONISHI M. Comparative neurophysiological studies of hearin and vocalization in songbirds. Z. vergl. Physiol. 66:257–272, 1970.

LEVIN MD, KUBKE MF, SCHNEIDER M, WENTHOLD R, CARR CE. Localization of AMPA-selective glutamate receptors in the auditory brainstem of the barn owl. J. Comp. Neurol. 378:239–253, 1997.

MOISEFF A. Binaural disparity cues available to the barn owl for sound localization. J. Comp. Physiol. A 164:629–636, 1989.

RHODE WS, GREENBERG S. Physiology of the cochlear nuclei. Popper AN, Fay RR, The Mammalian Auditory Pathway: Neurophysiology. Springer-Verlag New York 1992, 94–152.

SACHS MB, SINNOTT JM. Responses to tones of single cells in Nucleus magnocellularis and Nucleus angularis of the Redwing Blackbird (*Agelaius phoeniceus*). J. Comp. Physiol. 126:347–361, 1978.

SOARES D, CARR CE. The cytoarchitecture of the nucleus angularis of the barn owl (*Tyto alba*). J. Comp. Neurol. 429:192–205, 2001.

SULLIVAN WE. Classification of response patterns in cochlear nucleus of barn owl: Correlation with functional response properties. J. Neurophysiol. 53:201–216, 1985.

SULLIVAN WE, KONISHI M. Segregation of stimulus phase and intensity coding in the cochlear nucleus of the barn owl. J. Neurosci. 4:1787–1799, 1984.

TAKAHASHI TT, KONISHI M. Projections of the cochlear nuclei and nucleus laminaris to the inferior colliculus of the barn owl. J. Comp. Neurol. 274:190–211, 1988.

TAKAHASHI T, MOISEFF A, KONISHI M. Time and intensity cues are processed independently in the auditory system of the owl. J. Neurosci. 4:1781–1786, 1984.

TRUSSELL LO. Cellular mechanisms for preservation of timing

in central auditory pathways. Curr. Opin. Neurobiol. 7:487–492, 1997.

WARCHOL ME, DALLOS P. Neural coding in the chick cochlear nucleus. J. Comp. Physiol. A 166:721–734, 1990.

WHITEHEAD MC, MOREST DK. Dual populations of efferent and afferent cochlear axons in the chicken. Neuroscience 6:2351–2365, 1981.

WINTER P. Vergleichende qualitative und quantitative Untersuchungen an der Hörbahn von Vögeln. Z. Morphol. Ökol. Tiere 52:365–400, 1963.